Deriving Electrophysiological Brain Network Connectivity via Tensor Component Analysis During Freely Listening to Music

Yongjie Zhu, *Student Member, IEEE*, Jia Liu, *Student Member, IEEE*, Klaus Mathiak, Tapani Ristaniemi, *Senior Member, IEEE*, and Fengyu Cong, *Senior Member, IEEE*

***Abstract*— Recent studies show that the dynamics of electrophysiological functional connectivity is attracting more and more interest since it is considered as a better representation of functional brain networks than static network analysis. It is believed that the dynamic electrophysiological brain networks with specific frequency modes, transiently form and dissolve to support ongoing cognitive function during continuous task performance. Here, we propose a novel method based on tensor component analysis (TCA), to characterize the spatial, temporal, and spectral signatures of dynamic electrophysiological brain networks in electroencephalography (EEG) data recorded during free music-listening. A three-way tensor containing time-frequency phase-coupling between pairs of parcellated brain regions is constructed. Nonnegative CANDECOMP/PARAFAC (CP) decomposition is then applied to extract three interconnected, low-dimensional descriptions of data including temporal, spectral, and spatial connection factors. Musical features are also extracted from stimuli using acoustic feature extraction. Correlation analysis is then conducted between temporal courses of musical features and TCA components to examine the modulation of brain patterns. We derive several brain networks with distinct spectral modes (described by TCA components) significantly modulated by musical features, including higher-order cognitive, sensorimotor, and auditory networks. The results demonstrate that brain networks during music listening in EEG are well characterized by TCA components, with spatial patterns of oscillatory phase-synchronization in specific spectral modes. The proposed method provides evidence for the time-frequency dynamics of brain networks during free music listening through TCA, which allows us to better understand the reorganization of electrophysiological networks.**

***Index Terms*— Tensor decomposition, frequency-specific brain connectivity, freely listening to music, oscillatory coherence, electroencephalography (EEG).**

I. Introduction

THE electrophysiological network, characterized by neuronal synchronization between spatially separate brain regions, plays an important role in the human cognition [1], [2]. Such neuronal-synchronized networks are transient and dynamic, established on the specific frequency modes in order to support ongoing cognitive operations [3]–[7]. The characterization of the functional networks during resting state, referred to as resting-state brain networks (RSNs), has been widely studied during past few decades [8]–[10]. Recently, growing interest has been directed to probing the reorganization of brain functional networks during naturalistic stimuli [11]–[13] and a strong relationship between the functional networks during resting state and continuous task performance has been demonstrated [14], [15]. For example, Alavash and colleagues found that functional networks in challenging listening situations showed higher segregation of temporal auditory, ventral attention, and frontal control regions, compared to resting state [13]. Alluri et al. explored the neural correlates of music features processing as it occurs in a realistic or naturalistic environment [16], [17]. However, those functional connectivity studies have been based on functional magnetic resonance imaging (fMRI), which is indirect assessments of brain activity. Actually, little is known about how oscillatory basis is involved in the brain network activity during music listening. In this paper, we develop a tensor-based method which allows us to characterize the spatial, temporal, and spectral signatures of electrophysiological brain network connectivity using electroencephalography (EEG) recorded during freely listening to music.

Tensor component analysis (TCA), as a well-established tool for signal processing and machine learning [18]–[20],

Manuscript received August 29, 2019; revised November 5, 2019; accepted November 13, 2019. Date of publication December 18, 2019; date of current version February 12, 2020. This work was supported in part by the National Natural Science Foundation of China under Grant 91748105 and Grant 81471742, in part by the Fundamental Research Funds for the Central Universities under Grant DUT2019, in part by the Dalian University of Technology in China, and in part by the Scholarship from China Scholarship Council under Grant 201600090042 and Grant 201600090044. The work of Y. Zhu was supported by the Mobility Grant from the University of Jyväskylä. *(Corresponding author: Fengyu Cong.)*

Y. Zhu is with the School of Biomedical Engineering, Faculty of Electronic Information and Electrical Engineering, Dalian University of Technology, Dalian 116024, China, with the Faculty of Information Technology, University of Jyväskylä, 40014 Jyväskylä, Finland, and also with the Department of Psychiatry, Psychotherapy and Psychosomatics, Medical Faculty, RWTH Aachen University, 52074 Aachen, Germany.

J. Liu and F. Cong are with the School of Biomedical Engineering, Faculty of Electronic Information and Electrical Engineering, Dalian University of Technology, Dalian 116024, China, and also with the Faculty of Information Technology, University of Jyväskylä, 40014 Jyväskylä, Finland (e-mail: cong@dlut.edu.cn).

K. Mathiak is with the Department of Psychiatry, Psychotherapy and Psychosomatics, Medical Faculty, RWTH Aachen University, 52074 Aachen, Germany.

T. Ristaniemi is with the Faculty of Information Technology, University of Jyväskylä, 40014 Jyväskylä, Finland.

Digital Object Identifier 10.1109/TNSRE.2019.2953971

has shown to be powerful for neuroimaging data processing and analysis in cognitive neuroscience [21]–[26]. A tensor is a multi-dimensional representation of data or a multi-way array. Each dimension in the tensor is called a way or mode. For a matrix, a two-way array, matrix decomposition (e.g., independent component analysis, ICA) can be used for data processing. Analogously, for a tensor, tensor decomposition (or TCA) is able to be applied as well. TCA can reveal the true underlying structure of multi-way data and explore the interactions among multiple modes. For instance, TCA-based methods have been successfully applied to EEG data which is in general represented in time, frequency, and space [23]. In fMRI studies, the tensor modes could correspond to voxels, time, and patients [27]. In neurophysiological studies, the different modes could span neurons, time, and trials [28]. TCA can unsupervised uncover the main features of the neuroimaging data and extract low-dimensional descriptions of the big data. Several TCA-based modes have been used for decomposition and extraction of multi-way representation of data. The CANDECOMP/PARAFAC (CP) [29] is one of the fundamental models for tensor decomposition, which is a generalization of singular value decomposition (SVD) to higher-order tensor. TCA with CP model decomposes the multi-dimensional data into sum of rank-1 tensors of lower dimensions. Therefore, it can be applied to extract multi-interconnected and low-dimensional descriptions of original data. For example, performing TCA to the time-frequency transformed multi-channel EEG tensor, three interacted low-dimensional descriptions of data are extracted, including temporal factor representing temporal evolution of the oscillatory source, spectral factor representing oscillatory frequency, and the spatial factor representing location of the oscillatory source [30]. It should be noted that time-frequency representation of EEG data is usually nonnegative and CP decomposition with nonnegative constraints is adopted. Previous TCA-based studies of brain connectivity mainly focused on the aim of detection of change points [31]–[34] and spatial-temporal properties of the network community [35]–[37]. The spectral mode of brain networks was not considered especially for the fMRI neuroimaging data. Thus, these studies failed to examine the underling spectral mode of oscillatory networks. However, dynamics of large-scale networks during task performance have been shown to fluctuate across different frequency bands [6], [38]. For example, using magnetoencephalography (MEG), self-peace motor task studies demonstrated that the motor networks measured by the correlation of band-limited power is dominant in beta band [38], [39]. Further, few studies have attempted to explore spectral patterns of the brain functional connectivity during continuous task performance.

In this paper, we examined the spatio-temporal-spectral modes of covariation among separate regions in the listening brain. We recorded the EEG data during freely listening to music. Source-level data was obtained by source localization based on minimum-norm estimate. We then computed the time-frequency domain connectivity between all pairs of separate brain regions predefined though cortical parcellation, based on a sliding window technique. We used the weighted phase lag index (wPLI) as a metric to quantify the brain connectivity since it is insensitive to signal leakage and similar bias effects [40], [41]. We were able to obtain an adjacency matrix for each time window and frequency point. We reshaped the upper triangular parts of adjacency matrix into a vector. We then constructed a three-way tensor containing time, frequency, and connectivity modes for each subject. We performed CP decomposition on the temporal-concatenated adjacency tensor for multi-subjects. It should be noted that it is distinct from our previous study [5], where CP decomposition was applied to time-frequency representations of source-level EEG data. In the present study, we extracted low-dimensional, spatio-temporal-spectral modes of covariation including connectivity factor reflecting network community, temporal factors reflecting temporal evolution of functional networks and the spectral factors reflecting spectral features of networks. Time series of five long-term acoustic feature were extracted from the audio stimuli by music information retrieval techniques used in previous studies [17], [42]. Finally, we analyzed the correlation between temporal courses and the musical feature time series to identify frequency-specific brain networks modulated by musical features.

II. Material and Methods

A. Data Description

We used EEG data of 14 right-hand adults aged 20 to 46 years old. None of them reported hearing loss or history of neurological disease. No participants had musical expertise. This study was approved by the local ethics committee. During the experiment, participants were presented with a music played through audio headphones. This music was a 512 s long musical clips of modern tango, which had suitable duration for the experimental setting due to its high range of fluctuation in several musical features [17]. EEG data were recorded at a sampling rate of 2048 Hz with BioSemi electrode caps of 64-channels while participants were freely listening to musical clip.

Here, we examined five acoustic features including tonal and rhythmic features. They were extracted by applying a frame-by-frame analysis technique [17], [42]. The length of each frame was set as 3 seconds and the overlap between adjacent frames was set as 2 seconds. Thus, one temporal course with 510 samples was created for each musical feature with a sampling rate of 1 Hz. The five acoustic features consist of two tonal musical feature, Mode and Key Clarity, and three rhythmic features, including Fluctuation Centroid, Fluctuation Entropy and Pulse Clarity. Mode denotes the strength of major or minor mode. Key Clarity represents the measure of the tonal clarity. Fluctuation Centroid is defined as the geometric mean of the fluctuation spectrum, indicating the global repartition of rhythm periodicities within the range of 0–10Hz [17]. Fluctuation entropy is the Shannon entropy of the fluctuation spectrum, representing the global repartition of rhythm periodicities. Pulse Clarity naturally estimates the clarity of the pulse.

B. Preprocessing and Source Reconstruction

We re-referenced EEG data using common average electrodes. We visually inspected for rejecting artifacts and bad

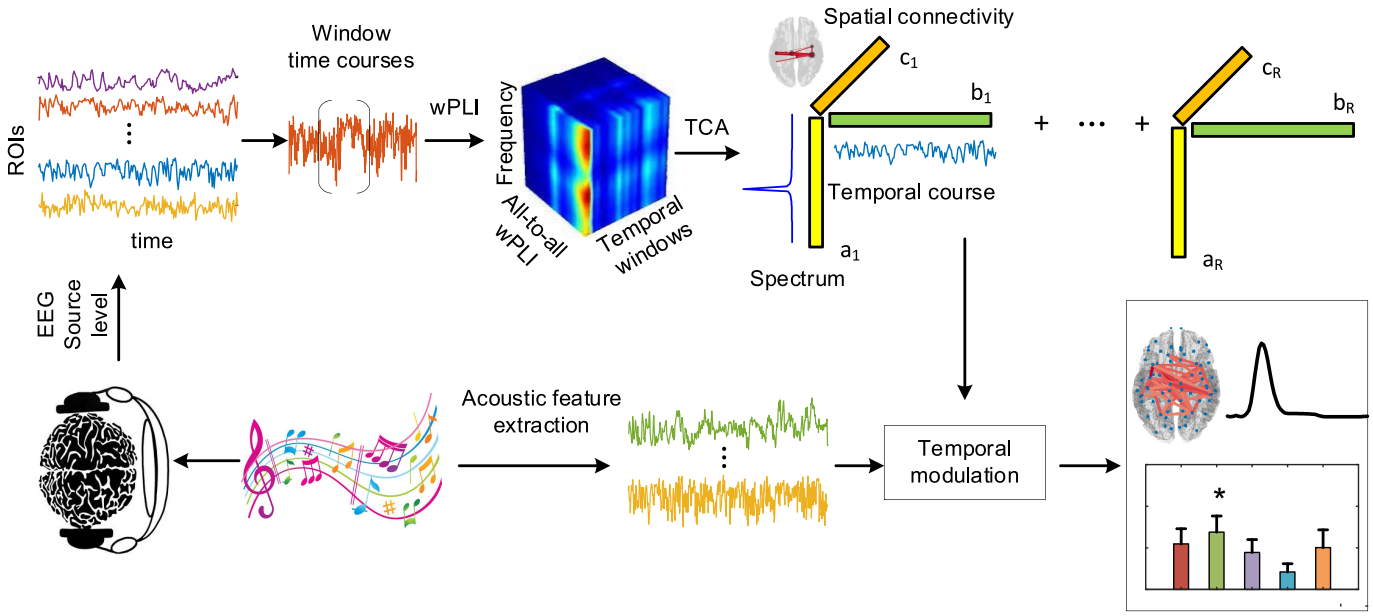

Fig. 1. Analysis pipeline. EEG data were recorded during freely listening to music. Source-reconstructed data were divided into 68 ROIs based on anatomical brain regions. Each windowed signal was transformed with a Morlet wavelet and wPLI was calculated between all pairs of ROIs. For each time window and frequency-point, an adjacent matrix was thus obtained. Then a three-way tensor was formed including spectral mode, temporal mode, and spatial connectivity mode (vectorized using upper triangular parts of an adjacent matrix). Nonnegative CP decomposition was applied to the temporally concatenated tensor across subjects. On the other hand, musical features were extracted using acoustic feature extraction. The temporal courses of decomposed components and musical feature time series were analyzed to examine the modulated brain networks.

channels were interpolated with mean value of their spherical adjacent channels. A 50 Hz notch filter was applied to remove powerline interference. High-pass and low-pass filters with 2 Hz and 35 Hz cutoff were then used since our previous investigation of the frequency range uncovered that no useful information was observed in higher frequencies [12], [42]. The data were finally down-sampled to 256 Hz. Independent component analysis (ICA) was performed on individual EEG data to remove EOG (e.g. eye blinks) [43]. A schematic of the subsequent data processing is demonstrated in Fig. 1. Following data preprocessing, the forward model and inverse model were computed using a MATLAB toolbox Brainstorm [44]. The symmetric boundary element method (BEM) was used to calculate the forward model with a default MNI MRI template (Colin 27). To solve the inverse model, weighted minimum-norm estimate (wMNE) [45] was applied, which is well-suited for estimation for brain connectivity since it takes the volume conduction into consideration and reduces single leakage [3]. The source orientations were constrained to be normal to the brain cortical surface when calculating the inverse problem. Then, the cortical surface was parcellated into 68 anatomical regions based on the Desikan-Killiany Atlas (DKA) [46]. In order to obtain a representative time series for every region, the center of mass of each region was defined as seed voxel and used as a single representative location. Thus, for each subject, a source-level data matrix $\mathbf{P}$ was created with dimension $n_n \times n_s$, where $n_n = 68$ represents the number of anatomical regions and n_s represents the number of samples.

C. Dynamic Functional Connectivity Estimation

We attempt to examine the time-frequency dynamics of brain functional connectivity. This means that we require estimating connectivity between all pairs of DKA regions, as a function of time and frequency using a sliding-window technique [47], [48]. Firstly, source space data matrix $\mathbf{P}$ was segmented by overlapping time window. A single window data is denoted as $\boldsymbol{P}_w$ with dimensions $n_n \times f\tau$. Here, w represents window number, τ denotes the window length in seconds and f is sampling frequency. Hamming-window with $\tau = 3s$ and 2 s overlap of adjacent windows were set, resulting in a sampling rate of 1 Hz in temporal dimension. This sampling rate was in line with musical feature time series.

To calculate phase-coupling between all pairs of regions in frequency domain, spectral densities should be estimated. We applied continuous wavelet transform with Morlet wavelets to the segmented data $\boldsymbol{P}_w$. The Morlet wavelet contained 3 cycles at the lowest frequency (2 Hz) and the number of cycles was increasing up to 12 cycles at the highest frequency (35 Hz). This resulted in 42 linearly spaced frequency points. A four-way tensor was thus obtained with dimensions $n_n \times n_m \times n_f \times n_w$, where $n_w = 512$ denotes the number of windows, $n_f = 42$ is the number of frequency point and $n_m = f\tau$ is the number of samples in a single window.

Weighted phase lag index (wPLI) is defined as the sign of the phase difference between two signals weighted by the magnitude of the imaginary component of the cross-spectrum [41]. It is computed as

$$wPLI_{(f,w)} = \frac{|\sum_{t=1}^{f\tau} im\left(S_1^w(f,t)\, S_2^{w*}(f,t)\right)|}{\sum_{t=1}^{f\tau} |\, im\left(S_1^w(f,t)\, S_2^{w*}(f,t)\right)|}, \quad (1)$$

where $S_1^w(f,t)$ and $S_2^w(f,t)$ are wavelet-decomposed time-frequency representations from DKA region 1 and region 2 respectively, and segmentation w. $*$ means the complex

conjugate, $im(\ \ )$ represents the imaginary part of a complex value, $|\ \ |$ is an absolute value operation. Note that wPLI here descripts the degree of phase synchronization between regions in a period of time ($\tau = 3\ s$). After calculation of wPLI, for each subject, a three-way tensor containing connections $\boldsymbol{Q}$ was generated with dimensions $n_c \times n_w \times n_f$, where $n_c = 2278$ is the number of pairs of regions ($68 * (68-1)/2$). Finally, these three-way tensors $\boldsymbol{Q}$ were temporally concatenated across subjects, resulting in a group-level tensor $\boldsymbol{\mathcal{X}}$ with dimensions $n_c \times n_w n_p \times n_f$, where n_p is the number of subjects.

D. Learning Underlying Brain Networks via Tensor Decomposition

CP model, as a fundamental model for TCA, decomposes a tensor into multiple components through a high-order singular value decomposition. It has found many applications in several fields, especially for signal processing and machine learning [18], [19]. Given a three-way tensor $\boldsymbol{\mathcal{X}} \in \mathbb{R}_{+}^{n_c \times n_t \times n_f}$ from constructed tensor containing connectivity, a rank-R nonnegative CP mode factorizes $\boldsymbol{\mathcal{X}}$ into R components, each of which contains a rank-1 tensor produced by the outer-product of 3 column vectors. It is generally solved through the following minimization problem with Frobenius norm of the error:

$$\min_{A,B,C} \frac{1}{2} \left\| \boldsymbol{\mathcal{X}} - \sum_{r=1}^{R} \mathbf{A}_r \otimes \mathbf{B}_r \otimes \mathbf{C}_r \right\|_F^2, \tag{2}$$

where $\boldsymbol{A} = [\boldsymbol{a}_1, \boldsymbol{a}_2, \cdots, \boldsymbol{a}_R]$, $\boldsymbol{B} = [\boldsymbol{b}_1, \boldsymbol{b}_2, \cdots, \boldsymbol{b}_R]$, and $\boldsymbol{C} = [\boldsymbol{c}_1, \boldsymbol{c}_2, \cdots, \boldsymbol{c}_R]$ are called loading matrices or factor matrices. Here, those loading matrices represent connectivity factor matrix, spectral factor matrix, and temporal factor matrix respectively. $\|\ \ \|_F$ represents Frobenius norm. $\otimes$ means Kruskal operator. The estimated loading matrices with Kruskal operator form can be written as the sum of R rank-1 tensors with outer-product of column vectors form:

$$\sum_{r=1}^{R} \boldsymbol{A}_r \otimes \boldsymbol{B}_r \otimes \boldsymbol{C}_r = \sum_{r=1}^{R} \boldsymbol{a}_r \circ \boldsymbol{b}_r \circ \boldsymbol{c}_r, \tag{3}$$

where, $\boldsymbol{a}_r, \boldsymbol{b}_r$, and $\boldsymbol{c}_r$ character the spatio-temporal-spectral property of underling brain pattern. $\boldsymbol{a}_r$ can be considered as spatial topology of brain network pattern and $\boldsymbol{b}_r$ can be thought of as spectral mode of brain network pattern across oscillatory frequency. These spatial topology factors and spectral factors form structure that is common across time, which can be termed as frequency-specific brain network connectivity. The last set of factors $\boldsymbol{c}_r$ represent temporal factors of the underling brain pattern, which describes the temporal dynamic of such frequency-specific brain network connectivity. Since values of wPLI are nonnegative, we add a nonnegative constraint to Eq. (2), $\boldsymbol{a}_r \geq 0, \boldsymbol{b}_r \geq 0, \boldsymbol{c}_r \geq 0$.

There are many optimization algorithms for CP decomposition with nonnegative constraint, such as multiplicative updating (MU) method, alternating least squares (ALS) and hierarchical alternating least squares (HALS) [49]. Here, we apply ALS due to its good performance and fast speed on convergence. The ALS algorithm applies a gradient descent method to solve the minimization problem in Eq (2) iteratively. At each iteration, one factor matrix is updated while other two matrices are fixed. For brief illustration, consider estimating spatial topology matrix $\boldsymbol{A}$, fixing spectral factor matrix $\boldsymbol{B}$, and temporal matrix $\boldsymbol{C}$, which resulting in the following update rule:

$$\boldsymbol{A} \leftarrow \arg\min_{A} \frac{1}{2} \left\| \boldsymbol{\mathcal{X}} - \sum_{r=1}^{R} \boldsymbol{a}_r \circ \boldsymbol{b}_r \circ \boldsymbol{c}_r \right\|_F^2. \tag{4}$$

It can be estimated as a linear least-squares problem and has a closed-form solution. The solution of CP model using ALS algorithm is available in many open source toolboxes [50], [51].

E. Selection of Component Number

All TCA-based method for learning hidden data structures require determining the number of components either manually or via criteria such as DIFFIT method [52] and CORCONDIA method [53]. Indeed, DIFFIT and CORCONDIA measure the change of the data fitting (i.e. explained variance of the original data) and the core tensor of the decomposition among a number of models, respectively. It should be noted that the number of components R can be chose with a larger number than the minimization of each model size, which is not restricted by the size in each mode since the rank of tensor can be even larger than the max of each model size [29]. Here for simplicity, we use DIFFIT method to choose the number of components. DIFFIT, the difference in data fitting, is computed based on model reconstruction error and the explained variance of data [52], [54]. Let component number $R \in [1, \mathcal{R}]$, where $\mathcal{R}$ is the empirically maximal number of latent components. The data fit can be obtained as

$$Fit\,(R) = 1 - \frac{\left\| \boldsymbol{\mathcal{X}} - \sum_{r=1}^{R} \boldsymbol{a}_j \circ \boldsymbol{b}_j \circ \boldsymbol{c}_j \right\|_F}{\|\boldsymbol{\mathcal{X}}\|_F}. \tag{5}$$

Unlike PCA, the estimation of TCA may have local minima (suboptimal solution), and not guarantee that optimization routines will converge to the global optimal solution. Thus, we run ALS optimization procedure at each component number R 20 times from random initial conditions. We then average data fits across many runs, resulting in averaged data fit $\overline{Fit}(J)$. The change fit of two adjacent data fit is

$$DIF\,(R) = \overline{Fit}(R) - \overline{Fit}\,(R-1)\,. \tag{6}$$

Next, the ratio of the adjacent difference fits is defined as

$$DIFFIT\,(R) = \frac{DIF\,(R)}{DIF\,(R+1)}. \tag{7}$$

Generally, the candidate model $\tilde{R}$ with largest *DIFFIT* value is thought of as the appropriate model order of TCA for original tensor.

F. Modulation of Temporal Evolution by Musical Features

How does music modulate frequency-specific brain networks during real-world? We address this question for each

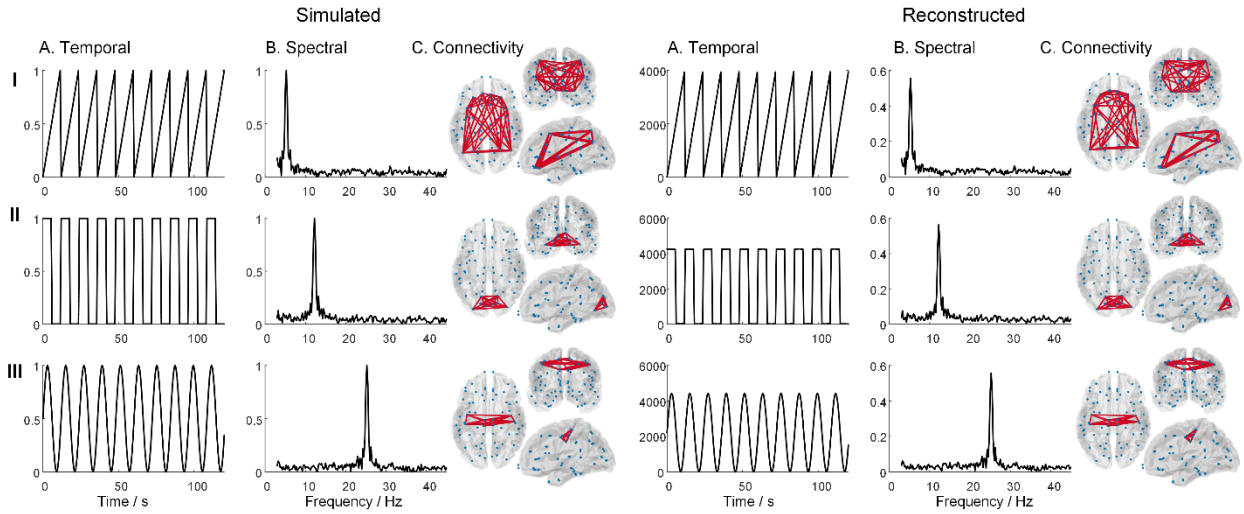

Fig. 2. Results for simulation. Left: the temporal, spectral, and spatial connectivity modes of three synthetic brain network patterns. Right: corresponding spectral and spatial connectivity modes of reconstructed brain patterns.

musical feature, temporal courses of brain networks (component) and subject. We aim to undertake a correlation analysis between temporal profile and musical time series, through evaluating the statistical significance of correlation based on a surrogate permutation procedure [55]. We obtained $\tilde{R}$ TCA components with three factors, charactering the temporal evolution, spectral mode, and spatial topology of brain networks. The temporal factor matrix $\boldsymbol{C}$ (with dimensions $n_w n_p \times \tilde{R}$) was firstly reshaped into a three-way tensor $\boldsymbol{\mathcal{C}}$ (with dimensions $n_w \times n_p \times \tilde{R}$), which includes individual temporal course for each component. For each component and each subject, we computed the correlation coefficient between each musical feature time series and temporal course as the modulation score. We then determined which component was significantly modulated by testing whether its modulation score was significantly different from the scores of surrogate data. The surrogate data were generated by a phase-randomization procedure [56], which rotated the intrinsic phase and preserved the properties of the temporal course in the spectral domain. We repeated the phase-randomization procedure 5000 times for each component. We calculated the correlation coefficient between musical feature time series and phase-randomized temporal courses to obtain a distribution of surrogate modulation scores. The 95$^{\text{th}}$ percentile ($p_{correct} = 0.05$) of surrogate modulation scores was selected as the threshold (control modulation scores for comparation) for each subject. Finally, for each component, we performed two-tailed t-tests for modulation score of each musical feature to determine which component (brain network pattern) was modulated significantly differently (at $p_{correct} = 0.05$ level) from the defined thresholds.

III. Results

A. Simulation Results

We firstly validated the proposed method using simulation data, which proved instructive to examine the performance of the methodology. The performance of wPLI, as a measure to examine functional connectivity in source space, has been validated well in previous study [40]. Thus, we here will not examine the performance of wPLI repeatedly. We only tested the ability of TCA, applied to time-frequency connectivity data, to character the temporal, spectral, and spatial changes in electrophysiological brain network over time scales of minutes.

We constructed an adjacency tensor $\boldsymbol{\mathcal{S}}_{sim}$ using outer product of temporal, spectral, and spatial topology factors of predefined true sources. The synthetic adjacency tensor was generated by $\boldsymbol{\mathcal{M}}_{sim} = \boldsymbol{\mathcal{S}}_{sim} + \boldsymbol{\mathcal{N}}_{sim} = \sum_{r=1}^{R} \boldsymbol{a}^r_{sim} \circ \boldsymbol{b}^r_{sim} \circ \boldsymbol{c}^r_{sim} + \boldsymbol{\mathcal{N}}_{sim}$, where $\boldsymbol{\mathcal{N}}_{sim}$ is a noise tensor with dimensions same as $\boldsymbol{\mathcal{S}}_{sim}$. Three distinct brain network patterns were predefined based on a previous work ($R = 3$), which consists of visual, sensorimotor, and fronto-parietal networks with distinct spectral modes [39]. Their temporal, spectral, and spatial topology profiles were shown in Fig. 2. Temporal factor matrix was constructed with triangle, square, and sine waves and spectral factor was composed of peaks at 5 Hz, 12 Hz and 25 Hz. We here demonstrated the results under the signal to noise ratio (SNR) of 10dB. As can be seen, the three underling true brain patterns with distinct temporal-spectral-spatial modes were successfully extracted using TCA.

B. Results From Music-Listening EEG Data

Figs. 3 and 4 demonstrate the identified brain network patterns (TCA components) during music listening: their spectral and spatial topology (connectivity) profiles, as well as their modulation by five musical features. The modulation score was averaged across subjects. Here, 25 components were extracted by CP decomposition according to DIFFIT method (See APPENDIX), and we presented 9 components that shown significant musical feature modulation. We observed two bilateral frontal functional networks, referred to as anterior higher-order cognitive brain networks in accordance with previous literature, but with distinct spectral modes (Rows I and II of Fig. 3). One of them is dominated by low-frequency oscillations

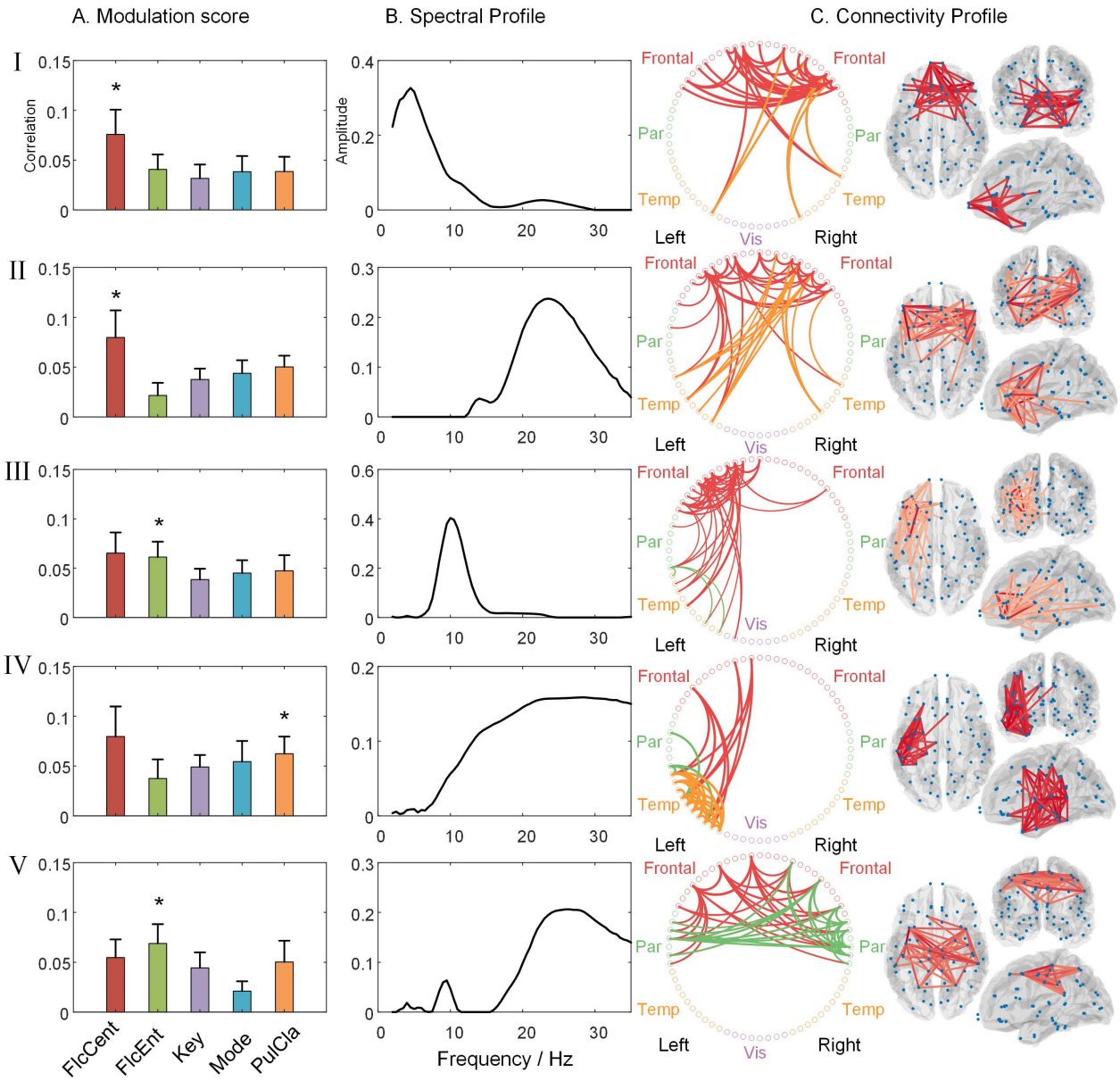

Fig. 3. Results for music-listening data. A. The modulation scores for each musical feature are computed from temporal course and averaged across subjects. Error bars represent standard errors of mean. An asterisk indicates that the component is modulated significantly differently from surrogate data. B. The spectral profiles are obtained from the spectral factor matrix. C. The circular phase-coupling plots and the 3D visualization of the connectivity profiles. Each node/dot represents one brain region. I. Anterior higher-order cognitive network with dominant delta/theta frequencies. II. Beta-specific higher-order cognitive network. III &IV. Language-related network with distinct spectral modes. V. Beta-specific motor network.

(Delta and Theta rhythms, 3-8 Hz) and another is centered at Beta rhythm (20-30 Hz). The regions involved by the two anterior higher-order cognitive networks are part of the default mode network (DMN), which here contains temporal poles, the ventromedial prefrontal cortex and posterior cingulate cortex. They are individually modulated by Fluctuation Centroid. Row III of Fig. 3 shows a 10 Hz unilateral functional networks, which mainly involves Broca's arears and temporal poles that are often associated with semantic integration. This brain pattern is significantly modulated by Fluctuation Entropy. Row IV of Fig. 3 shows a strong connectivity between temporal lobe and the frontal regions with a Beta-specific spectrum, which is significantly modulated by Pulse Clarity. We also found a Beta-specific sensorimotor component (Row V of Fig. 3), which involves regions including motor areas and is modulated by Fluctuation Entropy.

Fig. 4 demonstrates several brain connectivity networks mainly associated with auditory regions. The neural oscillations involved are dominated by Beta rhythm. Row I of Fig. 4 shows a bilateral temporal connectivity networks but no connections between left and right. The Beta rhythm was involved in this connectivity and it was modulated by Pulse Clarity. Rows II and III show strong connections between left temporal regions and right temporal regions with high-Beta

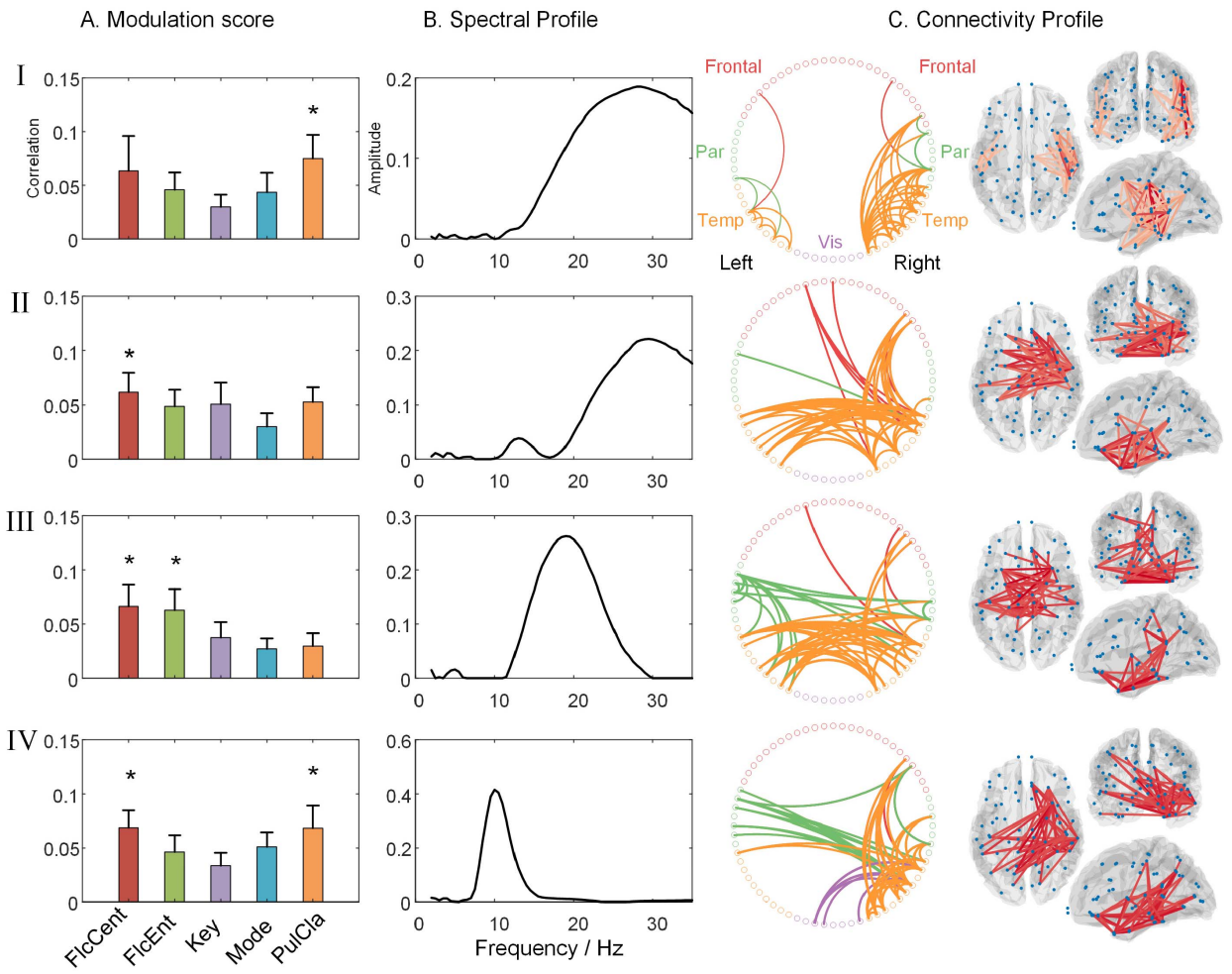

Fig. 4. Auditory-involved networks. I. Left and right temporal connectivity networks with dominant coherence in Beta range. II &III. Left to right temporal arears connections. IV. Alpha-specific right temporal network.

and low-Beta spectral modes. The temporal course of brain pattern in Row II is modulated by Fluctuation Centroid, as well as in Row III is modulated by both Fluctuation Centroid and Fluctuation Entropy. Row IV demonstrates connections between right temporal regions and left parietal regions. Its neural oscillations are dominated by Alpha rhythm (Peaks at 10 Hz) and its temporal course is significantly correlated with Fluctuation Centroid and Pulse Clarity.

IV. Discussion

In this paper, we introduced a TCA-based approach applied to EEG data, which allows us to characterize the time-frequency dynamics of electrophysiology networks during naturalistic music stimuli. We constructed a three-way tensor containing temporal evolution of frequency-specific functional connectivity in source space and used CP decomposition to extract the low-dimensional descriptions of brain networks. Using the proposed method, we extracted large-scale brain networks during freely listening to music, which was described by TCA components. Such TCA component, we refer to as a brain pattern, was pictured with a distinct spatially and spectrally defined pattern of network activity across the set of predefined-atlas regions spanning the whole brain. These patterns of frequency-specific phase-coupling were observed to be temporally modulated by musical feature time series and corresponded to plausible functional systems, including auditory, motor, and higher-order cognitive networks. As far as the authors are aware, this is the first complete formulation of an TCA-based approach for the analysis of electrophysiology network dynamics using ongoing EEG in source space during naturalistic and continuous music listening.

The two higher-order cognitive brain pattern (or networks) involved a subdivision of the DMN regions. These subdivisions had distinguishing features in different frequency bands, with one exhibiting high coherence in the Delta/Theta range (3–8 Hz) (Row I of Fig. 3) and the other showing a high coherence in the Beta range (20-30 Hz) (Row II of Fig. 3). The involved regions were composed of temporal poles, the ventromedial prefrontal cortex, and posterior cingulate cortex. Temporal poles are well believed to be related to semantic integration [6], [57] and the ventromedial prefrontal cortex is typically specialized for emotion regulation [58], which shows strong connection with the posterior cingulate cortex, a key region of the DMN [59]. Thus, the forming of these connectivity patterns is plausible to understand semantics expressed by music and induce related emotion during music

listening. For the neural oscillations, previous studies reported that cortical rhythm activity in the Beta range is related to behavioral performance during music listening and associated with predicting the upcoming note events [12], [60], which confirms our results that the frontal high-order networks with a high coherence in the Beta range emerged during music listening. In addition, the Delta-specific high-order cognitive network (Row I of Fig. 3) was also consistent with the previous studies, which showed that oscillations in the Delta played an important role in predicting the occurrence of auditory targets [61]. Rows III and IV of Fig. 3 demonstrated another two cognitive networks termed 'language network', one of which was specific to Fluctuation Entropy with a high coherence in Alpha band and another of which was modulated significantly by Pulse Clarity with a high coherence in Beta band. Previous studies revealed that brain functional networks engaged in music processing has strict similarities with that for language processing [62], [63]. Thus, the nodes of the language network including Broca's arears and the superior temporal sulcus, may be implicated during continuously listening to music. Recent spectral analysis techniques also demonstrated frequency-specific neural activity during processing language, where semantic and syntactic unification involves the alpha and beta bands by stronger recruitment of regions relevant for unification as indicated by the event-related desynchronization [64]. This study thus supports our findings that language network with strong coupling in alpha and beta bands emerged. For the motor networks (row V of fig. 4), it is believed that perception and execution of actions are strongly coupled in the brain as a result of learning a sensorimotor task, which facilitates not only predicting the action of others but also interacting with them [16]. During music listening, a tight coupling emerges between the perception and production of sequential information in hierarchical organization [16], [65]. Brain regions associated with motor networks may be involved due to the imitation and synchronization during musical activities (e.g. ensemble playing or singing). These networks involved in auditory areas (Fig. 4) showed beta-specific modes, which play an important function in music perception in agreement with previous studies [12], [17], [60].

TCA and other tensor analysis methods have been extensively examined from a theoretical perspective [29] and have been found quite many applications for the multi-way neuroimaging data in cognitive research [22], [28], [66]. The majority of studies have applied tensor decomposition to EEG and fMRI data, most typically to examine differences over subjects or time-frequency presentations of signals [23], [30], [67]. However, we do not find many applications regarding the characterization of temporal and spectral evolution of coupling between brain regions. Such coupling, generally termed functional connectivity, has been demonstrated temporal non-stationarity, spatial inhomogeneities, and spectral structure [38], [68]. It is natural to take into account the measure of time-frequency coupling between all pairs of regions based on wavelet transform, yielding a big data in tensor form with three modes corresponding to temporal course, spectrum, and spatial connectivity topology. TCA or tensor

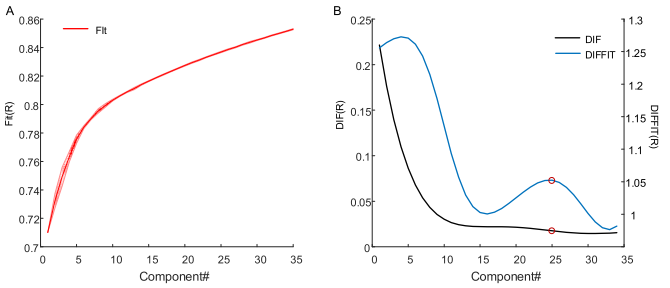

Fig. 5. The Fit, DIF, and DIFFIT curves in function of component R.

decomposition, as a simple extension of PCA, enables to process such high-dimensional data and extract low-dimensional components describing the interactions among modes. One of the key parameters for all TCA-based methods is the determination of component number to be modeled, which is less well prescribed and not a limitation of the proposed approach directly. In this paper, we used DIFFIT method to select the number of components. Note that DIFFIT provides a reference and instruction and is not able to accurately estimate the underlying true number of tensor components. We thus tried to vary this parameter (e.g., $R = from 20\ to 30$) in the current study and also observed the same networks significantly modulated by musical features as $R = 25$.

In addition to parameter selection, another common consideration is signal leakage through ill-posed inverse problem causing spurious correlations between signals. Here, we used wMNE algorithm, which is considered as an optimal source localization method for functional connectivity analysis [3]. Additionally, wPLI was applied to measure the phase coupling in time-frequency domain since it is insensitive to signal leakage and similar bias effects [4]. Yet, it should be noted that those techniques can only reduce the signal leakage problem, not overcome it completely.

Another issue is that we have only used one piece of naturalistic music stimuli to try to formulate an approach for analysis of functional connectivity dynamics during real-world. This work can be thought of as an exploratory study of neural basis of brain network during naturalistic task performance. Future work should adopt more musical clips and examine the repeatability of results. It is also possible to study the differences in brain network connectivity between resting state and music-listening.

V. Conclusion

In this paper, we introduced a data-driven approach to characterize the spatial, temporal, and spectral signatures of electrophysiological brain networks at source level across subjects during music listening. Previous studies have shown that brain connectivity is temporally non-stationary, dependent on frequency of oscillations and exhibit a degree of spatial inhomogeneity. The majority of methods for brain connectivity failed to examine the interactions among spatial, temporal, and spectral modes. Here, we apply TCA to the adjacent tensor constructed by time-frequency phase-coupling between pairs of brain regions. By doing so, we extract brain networks characterized by low-dimensional components with three factors. The temporal courses, representing the time evolution of

frequency-specific brain connectivity, are analyzed by correlation with time series of musical features extracted from music stimuli. We firstly validate the proposed method in simulation. Then we use it to the real EEG data recorded during free music listening. The identified brain networks with distinct spectral mode were in line with those previously published in the fMRI and EEG studies. The proposed method seems valuable for characterization of temporal and spectral evolution of coupling between brain regions during freely listening to music or other naturalistic stimuli.

Appendix

We run ALS optimization procedure at each component number R 20 times from random initial conditions. We then average data fits across many runs, resulting in averaged data fit (Fig. 5.A). Subsequently, the DIF, and DIFFIT were computed, as shown in Fig. 5.B. The DIT curve was smoothed by polynomial curve fitting since it usually fails to provide useful information due to fluctuations on DIF [30]. The two local maximums on DIFFIT curve at $R = 5$ and $R = 25$ indicate two positions on DIF curve that have fast dropping rate. Due to the low Fit value at the range $R < 15$, we selected the local maximum $R = 25$ as the appropriate model order.

The data used in the current study are available from the corresponding author on reasonable request and code to reproduce the simulation presented in this paper is available at *https://github.com/yongjiezhu/CPforBrainConnectivity.*

Acknowledgment

Y. Zhu thanks the Brain Imaging Facility of the Interdisciplinary Center for Clinical Research at RWTH Aachen University for providing the excellent working environment to write this article.

References

[1] K. J. Friston, "Functional and effective connectivity in neuroimaging: A synthesis," *Human Brain Mapping*, vol. 2, nos. 1–2, pp. 56–78, 1994.

[2] E. S. Finn *et al.*, "Functional connectome fingerprinting: Identifying individuals using patterns of brain connectivity," *Nature Neurosci.*, vol. 18, no. 11, p. 1664, 2015.

[3] M. Bola and B. A. Sabel, "Dynamic reorganization of brain functional networks during cognition," *Neuroimage*, vol. 114, pp. 398–413, Jul. 2015.

[4] A. Hillebrand, G. R. Barnes, J. L. Bosboom, H. W. Berendse, and C. J. Stam, "Frequency-dependent functional connectivity within resting-state networks: An atlas-based MEG beamformer solution," *Neuroimage*, vol. 59, no. 4, pp. 3909–3921, 2012.

[5] Y. Zhu, X. Li, T. Ristaniemi, and F. Cong, "Measuring the task induced oscillatory brain activity using tensor decomposition," in *Proc. IEEE Int. Conf. Acoust., Speech Signal Process. (ICASSP)*, May 2019, pp. 8593–8597.

[6] D. Vidaurre *et al.*, "Spontaneous cortical activity transiently organises into frequency specific phase-coupling networks," *Nature Commun.*, vol. 9, no. 1, p. 2987, 2018.

[7] C. Schmidt, D. Piper, B. Pester, A. Mierau, and H. Witte, "Tracking the reorganization of module structure in time-varying weighted brain functional connectivity networks," *Int. J. Neural Syst.*, vol. 28, no. 4, 2018, Art. no. 1750051.

[8] J. S. Damoiseaux *et al.*, "Consistent resting-state networks across healthy subjects," *Proc. Nat. Acad. Sci. USA*, vol. 103, no. 37, pp. 13848–13853, 2006.

[9] D. Mantini, M. G. Perrucci, C. Del Gratta, G. L. Romani, and M. Corbetta, "Electrophysiological signatures of resting state networks in the human brain," *Proc. Nat. Acad. Sci. USA*, vol. 104, no. 32, pp. 13170–13175, Aug. 2007.

[10] M. J. Brookes *et al.*, "Investigating the electrophysiological basis of resting state networks using magnetoencephalography," *Proc. Nat. Acad. Sci. USA*, vol. 108, no. 40, pp. 16783–16788, 2011.

[11] E. Simony *et al.*, "Dynamic reconfiguration of the default mode network during narrative comprehension," *Nature Commun.*, vol. 7, Jul. 2016, Art. no. 12141, doi: 10.1038/ncomms12141.

[12] Y. Zhu *et al.*, "Exploring frequency-dependent brain networks from ongoing EEG using spatial ICA during music listening," *bioRxiv*, Jan. 2019, Art. no. 509802.

[13] M. Alavash, S. Tune, and J. Obleser, "Modular reconfiguration of an auditory control brain network supports adaptive listening behavior," *Proc. Nat. Acad. Sci. USA*, vol. 116, no. 2, pp. 660–669, 2019.

[14] M. Demirtaş *et al.*, "Distinct modes of functional connectivity induced by movie-watching," *NeuroImage*, vol. 184, pp. 335–348, Jan. 2019.

[15] M. W. Cole, T. Ito, D. S. Bassett, and D. H. Schultz, "Activity flow over resting-state networks shapes cognitive task activations," *Nature Neurosci.*, vol. 19, no. 12, p. 1718, 2016.

[16] V. Alluri, P. Toiviainen, I. Burunat, M. Kliuchko, P. Vuust, and E. Brattico, "Connectivity patterns during music listening: Evidence for action-based processing in musicians," *Hum. Brain Mapping*, vol. 38, no. 6, pp. 2955–2970, 2017.

[17] V. Alluri, P. Toiviainen, I. P. Jääskeläinen, E. Glerean, M. Sams, and E. Brattico, "Large-scale brain networks emerge from dynamic processing of musical timbre, key and rhythm," *NeuroImage*, vol. 59, no. 4, pp. 3677–3689, 2012.

[18] N. D. Sidiropoulos, L. De Lathauwer, X. Fu, K. Huang, E. E. Papalexakis, and C. Faloutsos, "Tensor decomposition for signal processing and machine learning," *IEEE Trans. Signal Process.*, vol. 65, no. 13, pp. 3551–3582, Jul. 2017.

[19] A. Cichocki *et al.*, "Tensor decompositions for signal processing applications: From two-way to multiway component analysis," *IEEE Signal Process. Mag.*, vol. 32, no. 2, pp. 145–163, Mar. 2015.

[20] G. Zhou, A. Cichocki, Q. Zhao, and S. Xie, "Nonnegative matrix and tensor factorizations: An algorithmic perspective," *IEEE Signal Process. Mag.*, vol. 31, no. 3, pp. 54–65, May 2014.

[21] F. Cong *et al.*, "Benefits of multi-domain feature of mismatch negativity extracted by non-negative tensor factorization from EEG collected by low-density array," *Int. J. Neural Syst.*, vol. 22, no. 6, 2012, Art. no. 1250025.

[22] F. Cong *et al.*, "Multi-domain feature extraction for small event-related potentials through nonnegative multi-way array decomposition from low dense array EEG," *Int. J. Neural Syst.*, vol. 23, no. 2, 2013, Art. no. 1350006.

[23] F. Cong, Q.-H. Lin, L.-D. Kuang, X.-F. Gong, P. Astikainen, and T. Ristaniemi, "Tensor decomposition of EEG signals: A brief review," *J. Neurosci. Methods*, vol. 248, pp. 59–69, Jun. 2015.

[24] G. Zhou *et al.*, "Linked component analysis from matrices to high-order tensors: Applications to biomedical data," *Proc. IEEE*, vol. 104, no. 2, pp. 310–331, Feb. 2016.

[25] H. Lee, Y.-D. Kim, A. Cichocki, and S. Choi, "Nonnegative tensor factorization for continuous EEG classification," *Int. J. Neural Syst.*, vol. 17, no. 4, pp. 305–317, 2007.

[26] Y. Zhang, Q. Zhao, G. Zhou, J. Jin, X. Wang, and A. Cichocki, "Removal of EEG artifacts for BCI applications using fully Bayesian tensor completion," in *Proc. IEEE Int. Conf. Acoust., Speech Signal Process. (ICASSP)*, Mar. 2016, pp. 819–823.

[27] B. Hunyadi, P. Dupont, W. Van Paesschen, and S. Van Huffel, "Tensor decompositions and data fusion in epileptic electroencephalography and functional magnetic resonance imaging data," *Wiley Interdiscipl. Rev., Data Mining Knowl. Discovery*, vol. 7, no. 1, 2017, Art. no. e1197.

[28] A. H. Williams *et al.*, "Unsupervised discovery of demixed, low-dimensional neural dynamics across multiple timescales through tensor component analysis," *Neuron*, vol. 98, no. 6, pp. 1099–1115, 2018.

[29] T. G. Kolda and B. W. Bader, "Tensor decompositions and applications," *SIAM Rev.*, vol. 51, no. 3, pp. 455–500, 2009.

[30] D. Wang, Y. Zhu, T. Ristaniemi, and F. Cong, "Extracting multi-mode ERP features using fifth-order nonnegative tensor decomposition," *J. Neurosci. Methods*, vol. 308, pp. 240–247, Oct. 2018.

[31] A. G. Mahyari and S. Aviyente, "Identification of dynamic functional brain network states through tensor decomposition," in *Proc. IEEE Int. Conf. Acoust., Speech Signal Process. (ICASSP)*, May 2014, pp. 2099–2103.

[32] A. G. Mahyari, D. M. Zoltowski, E. M. Bernat, and S. Aviyente, "A tensor decomposition-based approach for detecting dynamic network states from EEG," *IEEE Trans. Biomed. Eng.*, vol. 64, no. 1, pp. 225–237, Jan. 2017.

[33] Y. Liu, J. Moser, and S. Aviyente, "Network community structure detection for directional neural networks inferred from multichannel multisubject EEG data," *IEEE Trans. Biomed. Eng.*, vol. 61, no. 7, pp. 1919–1930, Jul. 2014.

[34] S. B. Samdin, C.-M. Ting, H. Ombao, and S.-H. Salleh, "A unified estimation framework for state-related changes in effective brain connectivity," *IEEE Trans. Biomed. Eng.*, vol. 64, no. 4, pp. 844–858, Apr. 2017.

[35] A. Ozdemir, E. M. Bernat, and S. Aviyente, "Recursive tensor subspace tracking for dynamic brain network analysis," *IEEE Trans. Signal Inf. Process. Over Netw.*, vol. 3, no. 4, pp. 669–682, Dec. 2017.

[36] E. Al-sharoa, M. Al-khassaweneh, and S. Aviyente, "Tensor based temporal and multilayer community detection for studying brain dynamics during resting state fMRI," *IEEE Trans. Biomed. Eng.*, vol. 66, no. 3, pp. 695–709, Mar. 2019.

[37] M. Tang, Y. Lu, and L. Yang, "Temporal–spatial patterns in dynamic functional brain network for self-paced hand movement," *IEEE Trans. Neural Syst. Rehabil. Eng.*, vol. 27, no. 4, pp. 643–651, Apr. 2019.

[38] M. J. Brookes *et al.*, "Measuring temporal, spectral and spatial changes in electrophysiological brain network connectivity," *NeuroImage*, vol. 91, pp. 282–299, May 2014.

[39] G. C. O'Neill *et al.*, "Measurement of dynamic task related functional networks using MEG," *NeuroImage*, vol. 146, pp. 667–678, Feb. 2017.

[40] J. M. Palva *et al.*, "Ghost interactions in MEG/EEG source space: A note of caution on inter-areal coupling measures," *NeuroImage*, vol. 173, pp. 632–643, Jun. 2018.

[41] M. Vinck, R. Oostenveld, M. Van Wingerden, F. Battaglia, and C. M. A. Pennartz, "An improved index of phase-synchronization for electrophysiological data in the presence of volume-conduction, noise and sample-size bias," *NeuroImage*, vol. 55, no. 4, pp. 1548–1565, Apr. 2011.

[42] F. Cong *et al.*, "Linking brain responses to naturalistic music through analysis of ongoing EEG and stimulus features," *IEEE Trans. Multimedia*, vol. 15, no. 5, pp. 1060–1069, Aug. 2013.

[43] F. Cong, I. Kalyakin, T. Huttunen-Scott, H. Li, H. Lyytinen, and T. Ristaniemi, "Single-trial based independent component analysis on mismatch negativity in children," *Int. J. Neural Syst.*, vol. 20, no. 4, pp. 279–292, 2010.

[44] F. Tadel, S. Baillet, J. C. Mosher, D. Pantazis, and R. M. Leahy, "Brainstorm: A user-friendly application for MEG/EEG analysis," *Comput. Intell. Neurosci.*, vol. 2011, p. 8, Jan. 2011.

[45] F.-H. Lin, J. W. Belliveau, A. M. Dale, and M. S. Hämäläinen, "Distributed current estimates using cortical orientation constraints," *Hum. Brain Mapping*, vol. 27, no. 1, pp. 1–13, 2006.

[46] R. S. Desikan *et al.*, "An automated labeling system for subdividing the human cerebral cortex on MRI scans into gyral based regions of interest," *NeuroImage*, vol. 31, no. 3, pp. 968–980, Jul. 2006.

[47] B. Cai *et al.*, "Capturing dynamic connectivity from resting state fMRI using time-varying graphical lasso," *IEEE Trans. Biomed. Eng.*, vol. 66, no. 7, pp. 1852–1862, Jul. 2019.

[48] E. A. Allen, E. Damaraju, S. M. Plis, E. B. Erhardt, T. Eichele, and V. D. Calhoun, "Tracking whole-brain connectivity dynamics in the resting state," *Cerebral Cortex*, vol. 24, no. 3, pp. 663–676, 2014.

[49] A. Cichocki, R. Zdunek, A. H. Phan, and S.-I. Amari, *Nonnegative Matrix and Tensor Factorizations: Applications to Exploratory Multi-Way Data Analysis and Blind Source Separation*. Hoboken, NJ, USA: Wiley, 2009.

[50] B. W. Bader *et al. MATLAB Tensor Toolbox, Version [VERSION]*. Accessed: Jan. 7, 2012. [Online]. Available: https://www.tensortoolbox.org

[51] N. Vervliet, O. Debals, and L. De Lathauwer, "Tensorlab 3.0—Numerical optimization strategies for large-scale constrained and coupled matrix/tensor factorization," in *Proc. 50th Asilomar Conf. Signals, Syst. Comput.*, Nov. 2016, pp. 1733–1738.

[52] M. E. Timmerman and H. A. Kiers, "Three-mode principal components analysis: Choosing the numbers of components and sensitivity to local optima," *Brit. J. Math. Stat. Psychol.*, vol. 53, no. 1, pp. 1–16, 2000.

[53] R. Bro and H. A. L. Kiers, "A new efficient method for determining the number of components in PARAFAC models," *J. Chemometrics*, vol. 17, no. 5, pp. 274–286, 2003.

[54] M. Mørup and L. K. Hansen, "Automatic relevance determination for multi-way models," *J. Chemometrics, A J. Chemometrics Soc.*, vol. 23, nos. 7–8, pp. 352–363, 2009.

[55] D. Kim, K. Kay, G. L. Shulman, and M. Corbetta, "A new modular brain organization of the BOLD signal during natural vision," *Cerebral Cortex*, vol. 28, no. 9, pp. 3065–3081, 2017.

[56] D. Prichard and J. Theiler, "Generating surrogate data for time series with several simultaneously measured variables," *Phys. Rev. Lett.*, vol. 73, no. 7, p. 951, 1994.

[57] K. Tsapkini, C. E. Frangakis, and A. E. Hillis, "The function of the left anterior temporal pole: Evidence from acute stroke and infarct volume," *Brain*, vol. 134, no. 10, pp. 3094–3105, 2011.

[58] L. K. Fellows and M. J. Farah, "The role of ventromedial prefrontal cortex in decision making: Judgment under uncertainty or judgment per se," *Cerebral Cortex*, vol. 17, no. 11, pp. 2669–2674, 2007.

[59] M. E. Raichle, A. M. MacLeod, A. Z. Snyder, W. J. Powers, D. A. Gusnard, and G. L. Shulman, "A default mode of brain function," *Proc. Nat. Acad. Sci. USA*, vol. 98, no. 2, pp. 676–682, 2001.

[60] K. B. Doelling and D. Poeppel, "Cortical entrainment to music and its modulation by expertise," *Proc. Nat. Acad. Sci. USA*, vol. 112, no. 45, pp. E6233–E6242, 2015.

[61] L. H. Arnal, K. B. Doelling, and D. Poeppel, "Delta-beta coupled oscillations underlie temporal prediction accuracy," *Cerebral Cortex*, vol. 25, no. 9, pp. 3077–3085, 2014.

[62] L. Fadiga, L. Craighero, and A. D'Ausilio, "Broca's area in language, action, and music," *Ann. New York Acad. Sci.*, vol. 1169, no. 1, pp. 448–458, 2009.

[63] S. Koelsch, E. Kasper, D. Sammler, K. Schulze, T. Gunter, and A. D. Friederici, "Music, language and meaning: Brain signatures of semantic processing," *Nature Neurosci.*, vol. 7, no. 3, p. 302, 2004.

[64] N. H. L. Lam, J.-M. Schoffelen, J. Uddén, A. Hultén, and P. Hagoort, "Neural activity during sentence processing as reflected in theta, alpha, beta, and gamma oscillations," *NeuroImage*, vol. 142, pp. 43–54, Nov. 2016.

[65] I. Molnar-Szakacs and K. Overy, "Music and mirror neurons: From motion to'e'motion," *Social Cognit. Affect. Neurosci.*, vol. 1, no. 3, pp. 235–241, 2006.

[66] E. L. Mackevicius *et al.*, "Unsupervised discovery of temporal sequences in high-dimensional datasets, with applications to neuroscience," *eLife*, vol. 8, Feb. 2019, Art. no. e38471.

[67] C. I. Kanatsoulis, N. D. Sidiropoulos, M. Akçakaya, and X. Fu, "Regular sampling of tensor signals: Theory and application to FMRI," in *Proc. IEEE Int. Conf. Acoust., Speech Signal Process. (ICASSP)*, May 2019, pp. 2932–2936.

[68] F. Li *et al.*, "The dynamic brain networks of motor imagery: Time-varying causality analysis of scalp EEG," *Int. J. Neural Syst.*, vol. 29, no. 1, 2018, Art. no. 1850016.